Hindawi
International Journal of Antennas and Propagation
Volume 2019, Article ID 2613591, 11 pages
https://doi.org/10.1155/2019/2613591

Research Article

Wide-Angle Frequency Scanning Leaky Wave Antenna Loaded CSRR Patch Based on SSPP Transmission Line

Zihao Fu, Tianliang Zhang, Tianhai Wu, You Lan, Wenxing Huang, and Leilei He

School of Aeronautics and Astronautics, University of Electronic Science and Technology of China, Chengdu, China

Correspondence should be addressed to Tianliang Zhang; ztl@uestc.edu.cn

Received 27 November 2018; Revised 3 February 2019; Accepted 4 April 2019; Published 21 April 2019

Academic Editor: Rocco Guerriero

A novel composite left-and-right-composite-handed leaky wave antenna is proposed based on Spoof Surface Plasmon Polaritons slow-wave transmission line at microwave band in this paper. Wide-angle frequency scanning of the antenna is achieved by combining the slow-wave dispersion characteristics of Spoof Surface Plasmon Polaritons and the left-and-right-composite-handed characteristics of the complementary split ring resonator structure. The simulated and experimental results show that, with the increase of frequency, the radiation mode of the antenna gradually changed from slow-wave mode to fast-wave radiation mode, and the pattern changed continuously. The scanning region of the main beams proposed covers 110° in φ=0° plane when the frequency increases from 8GHz to 15GHz, and the gain of the antenna kept between 7dBi and 10.4dBi.

1. Introduction

Surface Plasmon Polariton (SPP) is a type of surface wave system whose permittivity is completely opposite between two different media. Because of the interaction between electrons and the incident field, electromagnetic wave can propagate along the surface direction with exponential attenuation perpendicular to the surface of a material interface. Metal materials have plasma characteristics in optical and infrared frequency band. Hence SPP is widely used in optical and infrared fields. Because the metal can be equivalent to the perfect conductor in the microwave and millimeter wave band, it is sometimes difficult to achieve SPP slow-wave transmission in the microwave and terahertz frequency band. In [1], however, periodic metal grooves are used to realize the equivalent plasma structure in the microwave frequency band. The quasi-surface wave transmission is realized. The equivalent transmission mode is realized by the periodic metal through-hole array in [2]. The circuit that uses the periodic structure to realize the equivalent plasma to transmit surface waves is called Spoof Surface Plasmon Polaritons (SSPP). In [3], a planar SSPP structure is realized by etching cyclic U-type patches on substrates to achieve low profile and miniaturization. Because of the advantageous application prospect of SPP in high frequency, the concept of SSPP has attracted many scholars to research since it was put forward. SSPP dispersion characteristics of one-dimensional periodic structures are researched in [4]. Reference [5] presents a method to analyze the dispersion and loss characteristics of SSPP in terahertz band. Considering the metal conductivity and high order mode effect of SSPP, this method is very accurate. Reference [6] analyzes the theoretical model of SSPP. In addition, more research is dedicated to using SSPP to achieve filter [7], power divider [8], and radiation [9] performance, etc. Reference [10] realizes the end fire of SSPP transmission line through gradual structure. There are also many researches dedicated to the design of leaky wave antennas based on SSPP transmission line [11–14].

Left-and-right-composite-handed (CRLH) material is also a concept introduced from optics. Propagation of electromagnetic waves in equivalent left-handed or right-handed media through periodic resonant structure has been introduced. In the leaky wave antenna, which loaded CRLH radiation structure, the backward wave radiation can be understood in the specific frequency band. Using complementary split ring resonator (CSRR) [15, 16] or interdigital capacitance (IDC) [17, 18] resonant structure, the left-handed radiation characteristics of leaky wave antenna can be properly realized.

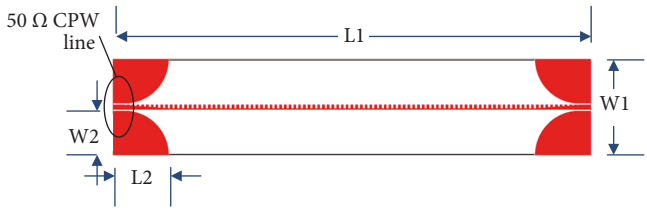

Figure 1: Layout of proposed SSPP.

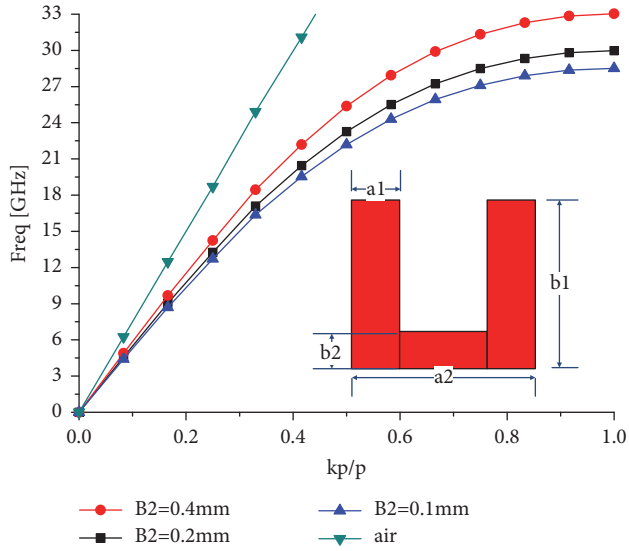

Figure 2: Comparison of dispersion curves between SSPP and air.

In this paper, a novel wide-angle frequency scanning CRLH leaky wave antenna based on SSPP transmission line is proposed. Combining the CRLH dispersion characteristics of CSRR resonators and the broadband characteristics of SSPP slow-wave transmission line, the CSRR resonates with the left-handed slow-wave band, the left-handed fast-wave band, and the right-handed fast-wave band successively by frequency scanning, and the 110° pattern main beam broadband scanning is realized. The simulated results match well with the measured results. In the frequency scanning region, the gain of the proposed antenna is kept within the range of 3.4dB.

2. SSPP Design

Unlike traditional microstrip lines, SSPP is an artificial surface wave transmission line that binds electromagnetic fields to metal surfaces through periodic metal structures, so there is no grounding part. Therefore, the coplanar waveguide (CPW) is more convenient to integrate with SSPP, to achieve impedance matching between connector and SSPP. This paper adopts the gradient matching circuit proposed in [19].

The layout of the SSPP transmission line is illustrated in Figure 1. By adjusting the size and spacing of the U-type metal patches, SSPP work is achieved in the target frequency band. Figure 2 shows the difference between the dispersion curve of the SSPP transmission line and the air dispersion curve by CST eigenmode solved. It can be seen from Figure 2 that with the decrease of B2, the slow-wave cutoff frequency of SSPP transmission line moved to a low frequency. When the dispersion curve slope is 0, the cutoff frequency of SSPP is reached. Because SSPP has the dispersion characteristics illustrated in Figure 2, with the increase of frequency, the phase change of SSPP increased in unit length. So, when SSPP is invoked as the feed transmission line of leaky wave antenna, the antenna has the characteristics of wide-angle scanning.

Figure 3 shows the electric field distribution of SSPP in slow-wave mode achieved by full wave simulation software HFSS. The electric field propagates in the direction of transmission and declines rapidly in the direction perpendicular to the transmission direction. It shows that the proposed SSPP has good electric field constraint.

3. CRLH Theory of CSRR

The layout and equivalent circuit of CSRR resonant structure of SSPP is shown in Figures 4 and 5. The CSRR equivalent circuit in Figure 5 can be divided into perfect left-handed (PLH) equivalent circuit and perfect right-handed (PRH) equivalent circuit. PRH can be equivalent to a series inductor and a parallel grounding capacitor as shown in Figure 5(a). The equivalent schematic diagram of PLH is obtained by PRH

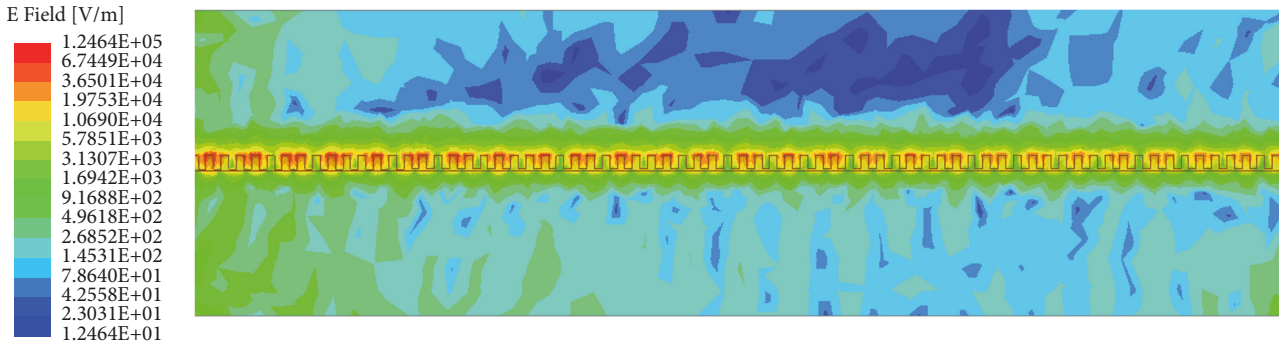

Figure 3: Electric field distribution of SSPP by HFSS.

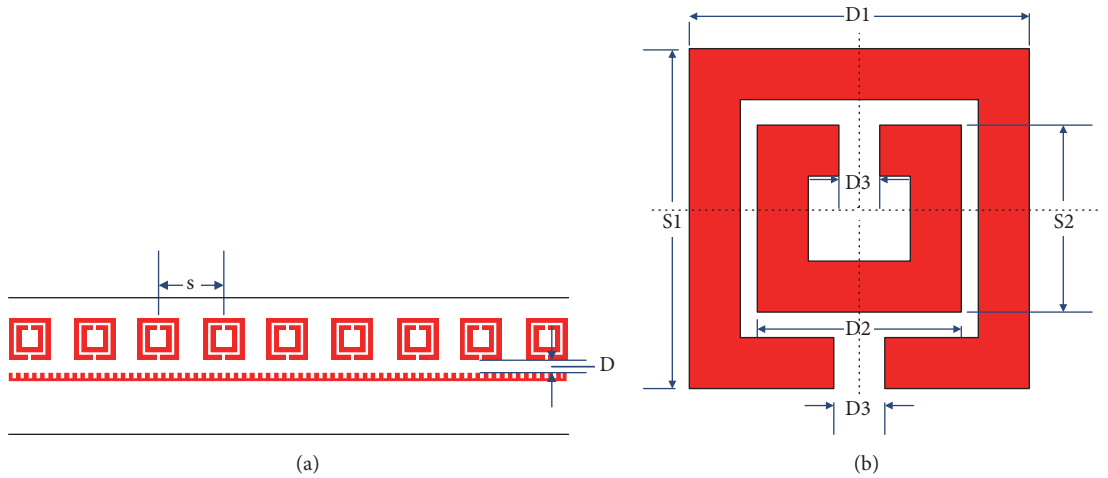

Figure 4: Layout of loading CSRR resonant structure. (a) Distribution of linear array. (b) Layout of CSRR.

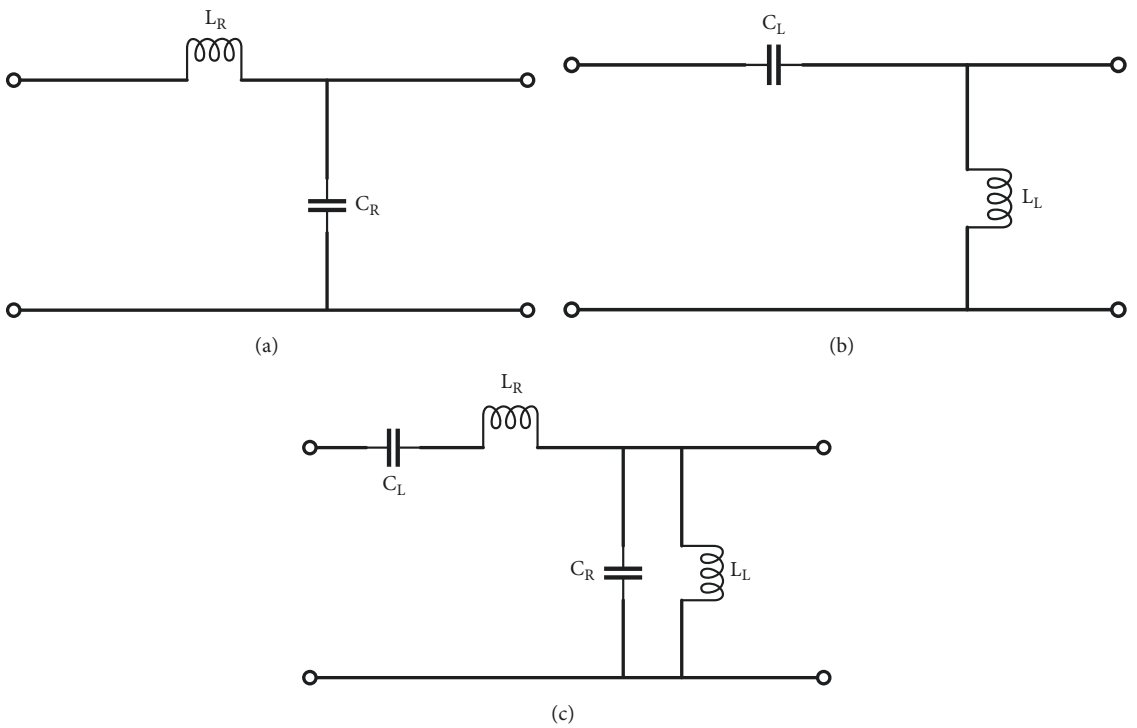

Figure 5: Equivalent schematic diagram. (a) Equivalent schematic diagram of PRH. (b) Equivalent schematic diagram of PLH. (c) Equivalent schematic diagram of CSRR.

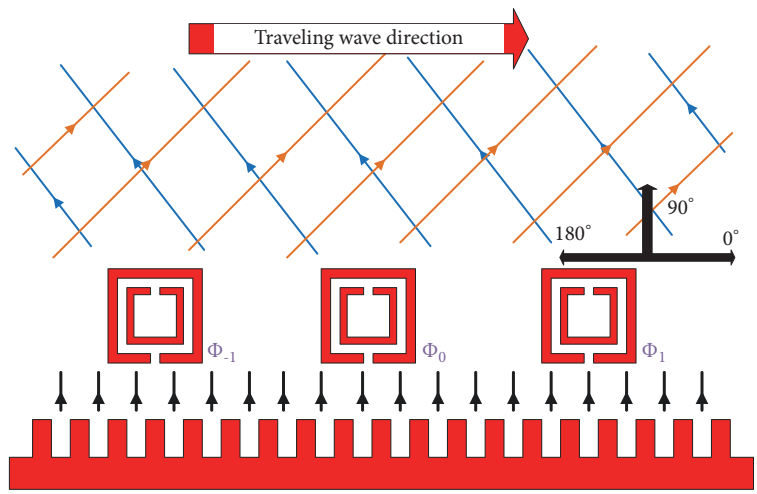

Figure 6: Working principle of proposed antenna.

duality principle, which is equivalent to series capacitor and parallel grounding inductance as shown in Figure 5(b).

The dispersion relation of CSRR can be obtained from (1).

$$\beta = \mathrm{s}(\omega)\sqrt{\omega^2 L_R C_R + \frac{1}{\omega^2 L_L C_L} - \left(\frac{L_R}{L_L} + \frac{C_R}{C_L}\right)} \quad (1)$$

$$\mathrm{s}(\omega) = \begin{cases} -1, & if\ \omega < \min\left(\dfrac{1}{\sqrt{L_R C_L}}\ and\ \dfrac{1}{\sqrt{L_L C_R}}\right) \\ +1, & if\ \omega > \max\left(\dfrac{1}{\sqrt{L_R C_L}}\ and\ \dfrac{1}{\sqrt{L_L C_R}}\right) \end{cases} \quad (2)$$

In (1), C_R and L_R are equivalent series capacitance and parallel inductance of CSRR. C_L and L_L are equivalent parallel capacitors and series inductors of CSRR. The cutoff frequencies of left-handed region and right-handed region are shown in formula (3) and (4) as follows:

$$\omega_{se} = \frac{1}{\sqrt{L_R C_L}} \quad (3)$$

$$\omega_{sh} = \frac{1}{\sqrt{L_L C_R}} \quad (4)$$

From formula (3) and (4), when $\sqrt{L_L/C_L} = \sqrt{L_R/C_R}$, $\omega_{se} = \omega_{sh}$, the dispersion of β is continuous. In this case, the state that conforms to the CRLH transmission lines is called the balanced state. When $\sqrt{L_L/C_L} \neq \sqrt{L_R/C_R}$, $\omega_{se} \neq \omega_{sh}$. Hence, there is a frequency stopband. In this case, the CRLH transmission line is unbalanced. From (1) and (2), the equivalent phase constant β is a function of frequency ω. When $\omega > \max(\omega_{se}, \omega_{sh})$, $\beta > 0$, CSRR is in the right-hand region. When $\omega < \min(\omega_{se}, \omega_{sh})$, $\beta < 0$, CSRR is in the left-hand region.

4. Wide-Angle Scanning Theory

Leaky wave radiation of SSPP can be realized by loading parasitic patches on the SSPP opening side [19–21]. Because of the slow-wave dispersion of SSPP transmission line, SSPP leaky wave antenna holds the characteristics of wideband frequency sweep. By loading CSRR patches, the leakage radiation of SSPP is achieved on the one hand. On the other hand, the dispersion characteristics of CSRR and SSPP determine that antennas emit forward radiation to backward radiation. Left-handed slow-wave radiation, left-handed fast-wave radiation, and right-handed fast-wave radiation can be realized, respectively, by loading CSRR resonant element in SSPP.

Figure 6 shows the working principle of the SSPP CRLH antenna. The radiation of the proposed antenna consists of two parts. First, energy of SSPP is spatially coupled to the CSRR radiation patches. Further, CSRR patches radiate energy into space. The radiation main beam direction of the antenna depends on the feed phase of SSPP and the compensation phase of CSRR. Feed phase Φ_i (i $= -1, 0, 1$) of SSPP changed with frequency increasing. Because of the change of feed frequency, the response mode of CSRR also changes. When CSRR's resonance mode n >0, CSRR has a positive electrical length; that is to say, CSRR's compensation phase φ_i is positive. When CSRR is in the left-handed band, its resonance mode n< 0. The electrical length of CSRR is negative and Φ_i is compensated negatively.

The compensation phase φ_i of CSRR is obtained by formula (5).

$$\varphi_i = \beta l = \frac{2\pi}{\lambda} n\pi = 2\mathrm{n}\pi \quad (5)$$

The radiation pattern of antenna can be obtained by formula (6) proposed in [19].

$$\mathrm{E} = \mathrm{C}\frac{e^{-jkr}}{r} f(\theta_r, \varphi) \sum_{n=-i}^{i} I_n e^{jn(kd\sin\theta_r + \Phi_i)} \quad (6)$$

Where $f(\theta, \varphi)$ is the radiation pattern of CSRR unit, θ_r is the scanning angle of proposed antenna. k is the wavenumber of proposed antenna.

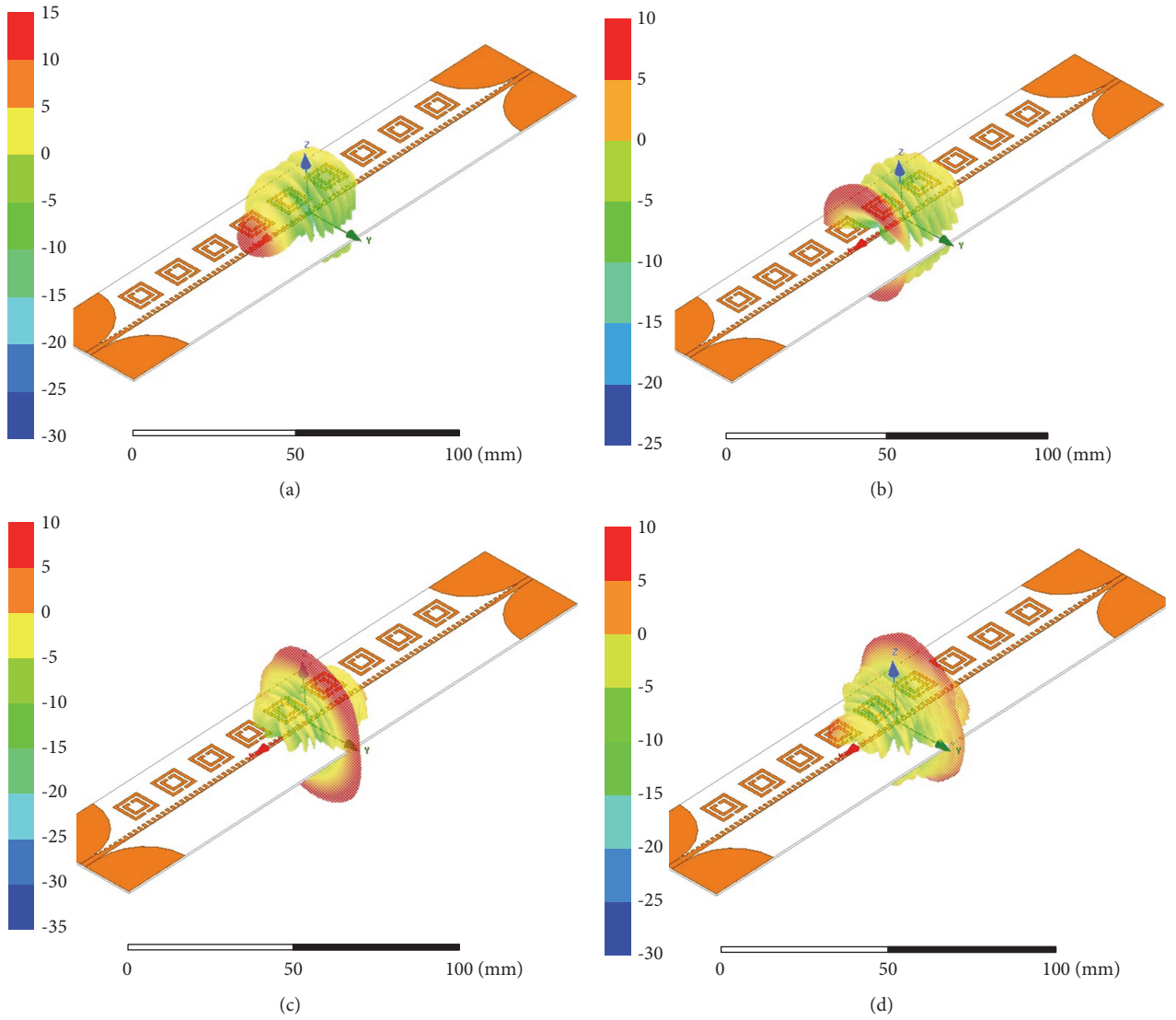

FIGURE 7: Antenna pattern in different dispersion regions. (a) Slow wave. (b) Left-handed fast wave. (c) Broadside. (d) Right-handed fast wave.

When $\Phi_i \in [-kd, 0]$, the main beam radiation direction $\theta_r = 90^\circ \sim 180^\circ$, antenna produces backward radiation. The radiation direction of proposed antenna is shown in the blue line in Figure 6. When $\Phi_i \in [0, kd]$, the main beam radiation direction $\theta_r = 0^\circ \sim 90^\circ$, antenna produces forward radiation. The radiation direction of proposed antenna is shown in the brown line in Figure 6, where d is the distance of the radiating elements.

Figure 7 shows the radiation field of the slow-wave (at 8GHz), left-hand fast-wave (at 10GHz), broadside (at 12.5GHz), and right-hand fast-wave (at 15GHz) radiation mode, respectively, by HFSS. It can be observed in Figure 7 that CSRR will support the slow-wave mode at a frequency point, and then it will no longer radiate in free space but will propagate along the surface wave delay transmission line, thus realizing the surface wave radiation. In Figure 7(a), the antenna is on the left-hand slow-wave region, so the radiation main beam is opposite to the traveling wave direction. Because the electrical length of CSRR increases at high frequencies, the CSRR cannot be equivalent to an ideal subwavelength resonant structure, so there is no right-handed slow-wave region of the proposed antenna.

The above theory is the principle of wide-angle scanning at the microscopy of the proposed antenna. Macroscopically, the wide-angle scanning characteristic of the proposed antenna is due to its dispersion in different regions. The dispersion curve of the antenna radiation element is illustrated in Figure 8. There is an open stopband between the slow-wave and fast-wave regions. Therefore, the gain of the proposed antenna at 9GHz to 10.5GHz will be attenuated.

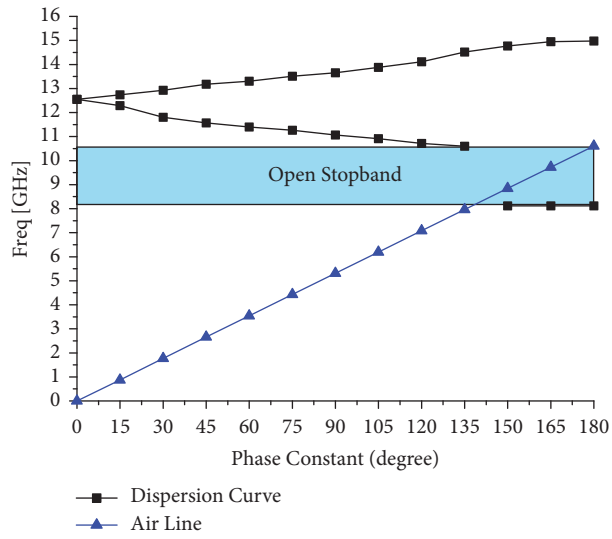

Figure 8: Dispersion curve of antenna radiation unit.

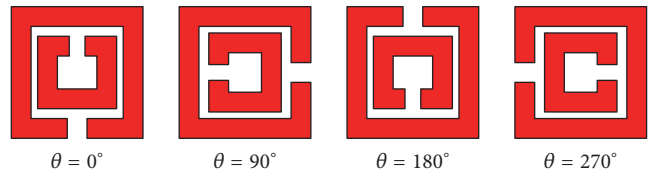

Figure 9: Deflection state of CSRR with θ changing.

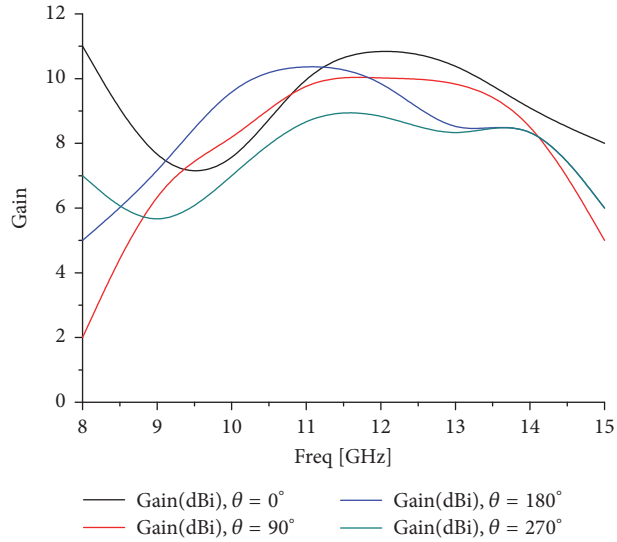

Figure 10: Influence of patch gap orientation on proposed antenna gain.

5. Parameter Study

The radiation characteristics of leaky wave antenna are directly affected by the dispersion of radiation element and the coupling between radiation element and the transmission line. Therefore, it is necessary to examine the coupling between the radiation element and the transmission line, the size of the patch, and the spacing between elements for the leaky wave antenna loaded with parasitic patches.

5.1. Patch Gap Orientation Factor. Deflection angle of CSRR resonator affects the coupling between transmission line and radiation element, so the influence of the deflection angle of antenna radiation should be considered. The CSRR structure corresponding to discrete theta values is shown in Figure 9. Figure 10 shows the relationship between CSRR patches deflection and the frequency sweep gain of the proposed antenna. It can be seen that the antenna gain fluctuates greatly during the frequency scanning process due to the asymmetry

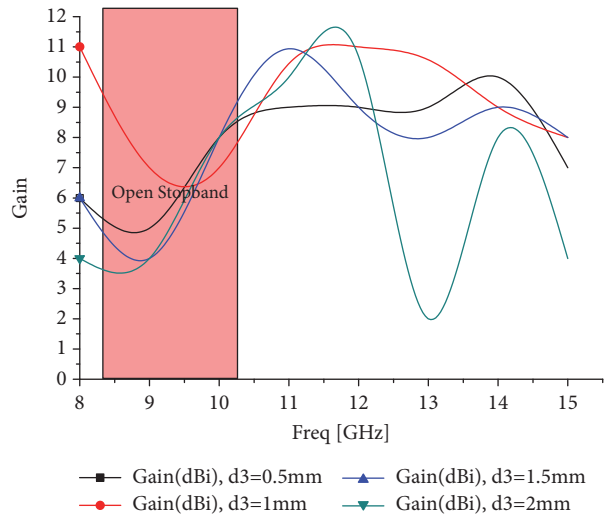

Figure 11: Influence of D3 on proposed antenna gain.

Table 1: Design parameters of the proposed antenna in Figure 11 (unit: mm).

L1	W1	L2	W2	S	D	A1	A2
191	40	23.86	18.86	16	3	0.5	2
S1	D1	S2	D2	D3	B1	B2	
10	10	8	8	1	2	0.2	

of CSRR patches in the direction of traveling wave when the patch rotates (±90°) and cannot be applied to the antenna design. When θ=0°, the antenna gain is higher and has a better consistency.

5.2. Gap Size Factor. As shown in Figure 8, the antenna has an open stopband between 9GHz and 10.5GHz. The value of D3 directly affects the value of equivalent C_R, $L_R C_L$, and L_L of CSRR. Then the resonance characteristics of CSRR are affected. As can be observed in Figure 11, the gain curve of the antenna decreases significantly from 8GHz to 10GHz, which is transition band from left-handed slow-wave region to left-handed fast-wave region. By adjusting D3, the gain from 8GHz to 9GHz can be effectively improved. When D3=1mm, the antenna gain fluctuates little.

5.3. Patch Size Factor. According to the above theory, the beam angle of the presented antenna is determined by φ_i and Φ_i together. However, the resonant frequency band of CSRR unit is limited. The effective radiation band of CSRR can be changed by enlarging the size of CSRR cell to n times of the original one. Figure 12 shows the deflection angle of the antenna beam with frequency when n = 0.5, 0.7, 1, and 1.3. When n = 1, the size of CSRR is shown in Table 1. Unmarked frequencies in the figure indicate that the maximum gain of the antenna is significantly reduced (> 4dB) or that the pattern has grating lobe.

When the frequency is constant, the compensation phase φ_i of the patch is constant, and the beam scanning step of the antenna is only related to the dispersion of the SSPP transmission line. As shown in Figure 2, when the dispersion characteristics of SSPP tend to slow wave, the step of phase Φ_i difference changed larger.

As shown in Figure 12, the beam direction of the proposed antenna is different in different frequency bands and is not linear. When the frequency is between 8 GHz and 9 GHz, the beam scanning step of the antenna reaches 48°/GHz. However, when the frequency is between 12GHz and 13GHz, the beam scanning step of the antenna reaches 6°/GHz. Therefore, when the effective radiation band of CSRR is in the frequency band with larger deflection step, the scanning angle of the proposed antenna increased accordingly. When the size of CSRR decreases, the applicable radiation band of antenna moves to high frequency. When n <1, the effective radiation frequency band of the antenna is higher than 9 GHz, and the pattern deflection angle is smaller. When n exceeds 1, the low cutoff frequency of the effective radiation band of the antenna is less than 8 GHz. At this point, the antenna is at the stop band, which reduces the scanning angle of the proposed antenna.

5.4. Coupling Factor. Figure 13 shows the effect of patch and SSPP transmission line spacing D of antenna return wave characteristic and gain. When D = 3mm, the average gain of the proposed antenna is the largest. When D becomes larger, the radiation efficiency of the proposed antenna is reduced. This phenomenon is explained by the weak coupling between CSRR and SSPP. Conversely, when D becomes smaller, the coupling between CSRR and SSPP becomes stronger, and matching between CSRR and SSPP transmission lines

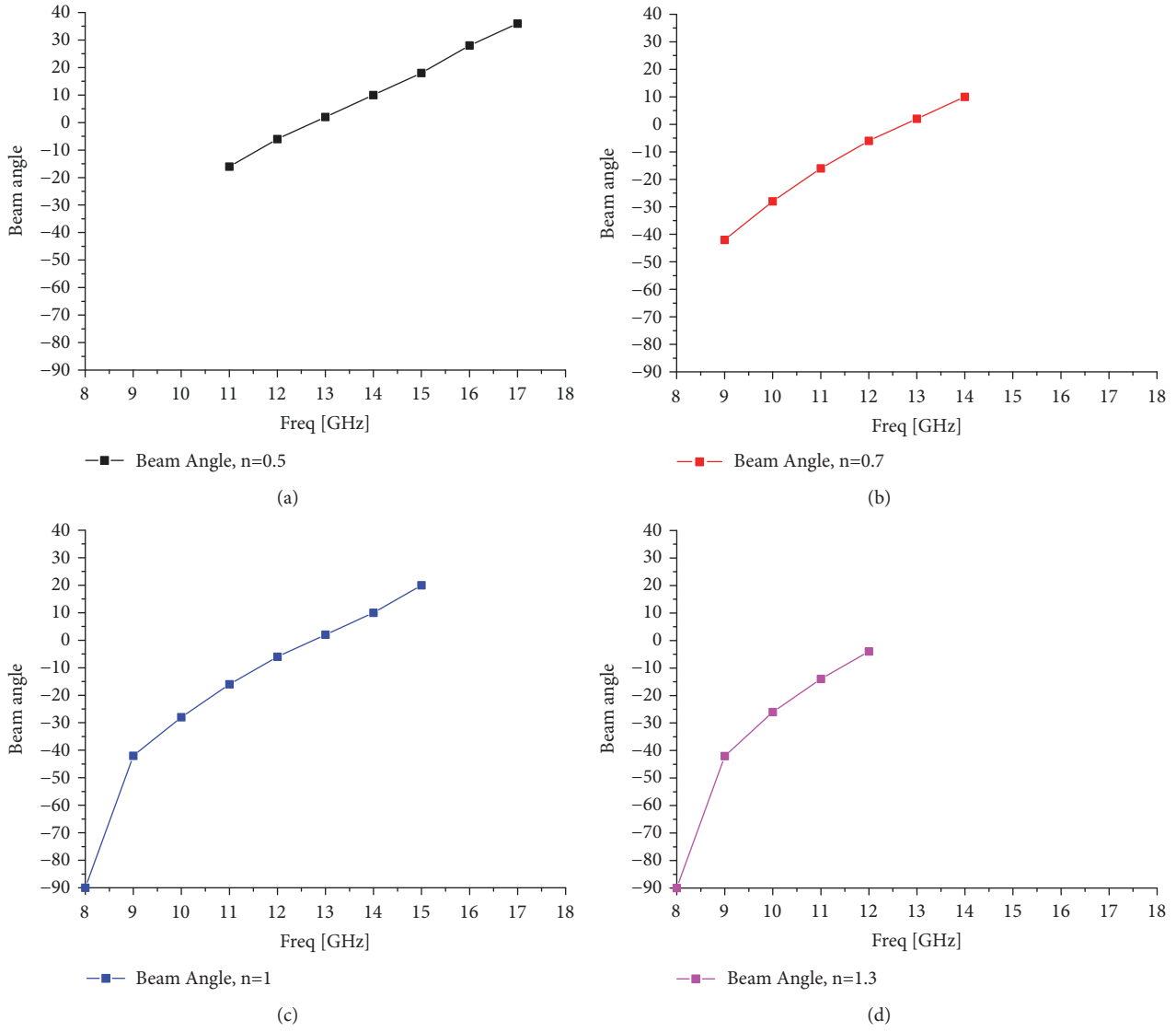

Figure 12: Influence of CSRR size on beam deflection angle. (a) n=0.5. (b) n=0.7. (c) n=1. (d) n=1.3.

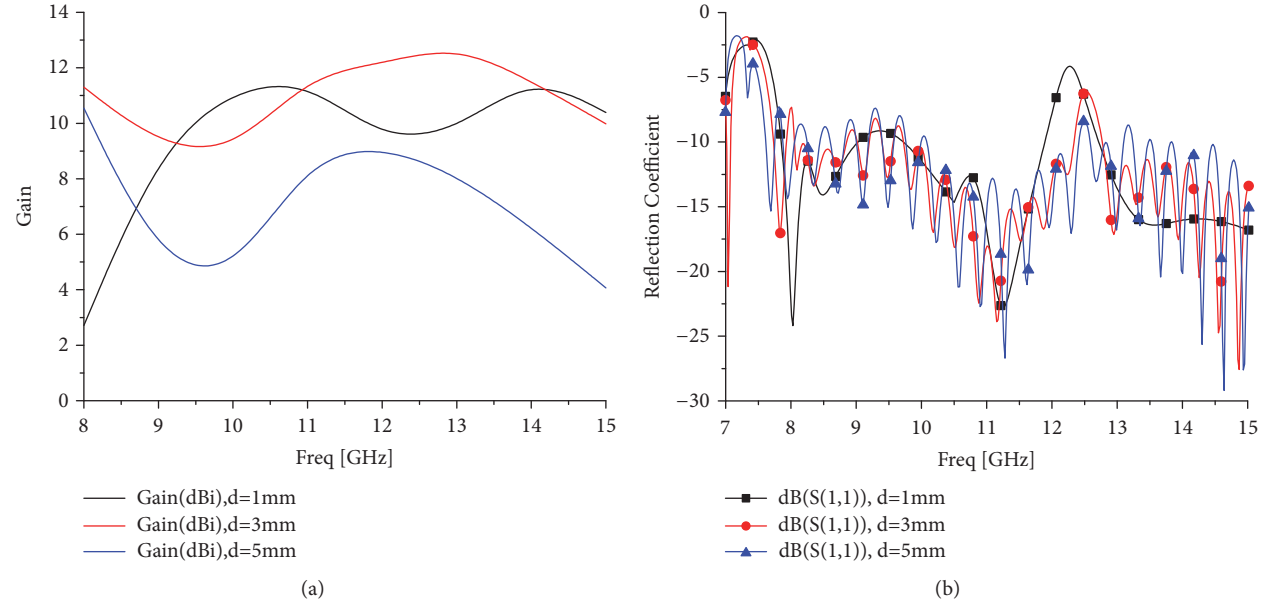

Figure 13: Influence of D on proposed antenna gain and reflection coefficient: (a) gain and (b) reflection coefficient.

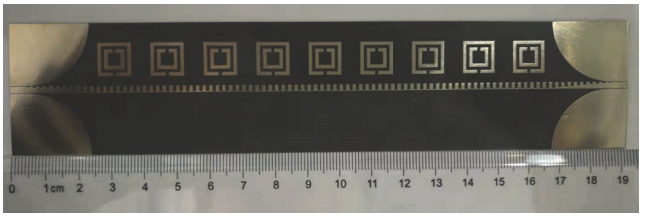

Figure 14: Photograph of proposed antenna.

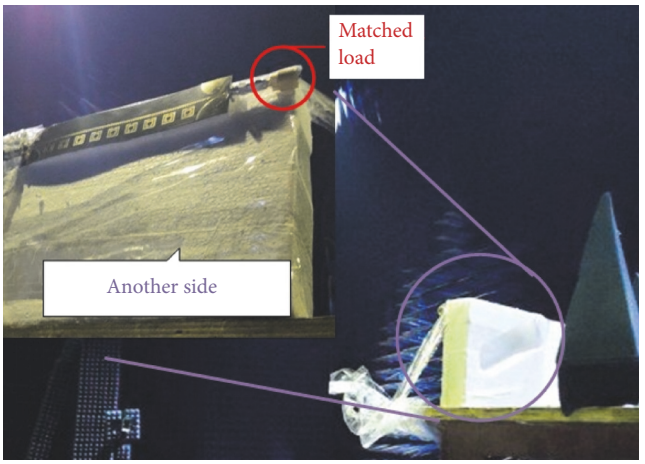

Figure 15: Measured environment of proposed antenna.

becomes worse. Therefore, the radiation gain of the antenna is also reduced.

6. Results and Discussion

Considering the constraints of measuring environment and assembly process, the length of the antenna is limited. Finally, a linear array composed of 9 CSRR patches is adopted in this paper. According to the above principle, the absolute size of the antenna is determined in Table 1. The circuit is etched on a Rogers 5880 substrate with a small dielectric constant ($\varepsilon = 2.2, \tan\delta = 0.0009$) to reduce the wave impedance between substrate and free space. The photograph of the proposed antenna is shown in Figure 14. Figure 15 shows the antenna pattern measured environment. Antenna was fed by the N5242a vector network analyser of Agilent Co during the measure.

The simulated and measured results of S parameters are presented in Figure 16. Figure 17 displays the simulated and measured results of the antenna normalized φ=0° plane pattern. The test platform reflected the electromagnetic radiation of the proposed antenna. Therefore, there are unnecessary side lobes and unevenness in the radiation pattern in Figure 17(b). When the antenna frequency changes from 8 GHz to 15 GHz, the antenna passes through the left-handed slow-wave region, left-handed fast-wave region, and right-handed region, and the φ=0° plane scanning angle achieves 110° wide-angle scanning. The gain of the proposed antenna remains between 7dBi and 10.4dBi from 8 to 15GHz. Figure 18 indicates the gain and main valve deflection angle of the antenna varied by frequency scanning.

7. Conclusions

In this paper, a novel wide-angle frequency scanning CRLH leaky wave antenna based on SSPP transmission line is presented. The antenna combines the slow-wave dispersion characteristic of SSPP and the CRLH characteristics of CSRR resonator to realize the wide-angle frequency scanning characteristics. By changing the frequency from 8GHz to 15GHz, the radiation mode of the antenna is modified into left-handed slow-wave region, left-handed fast-wave region, and right-handed fast-wave region successively. The pattern scanning of the main beam of the φ=0° plane is realized. Simulated results are in agreement with the measured results. The gain fluctuation is less than 3.4dB, and the direction of the main beam pattern changes 110° from 8GHz to 15GHz.

Data Availability

The data used to support the findings of this study are available from the corresponding author upon request.

Conflicts of Interest

The authors declare that there are no conflicts of interest regarding the publication of this article.

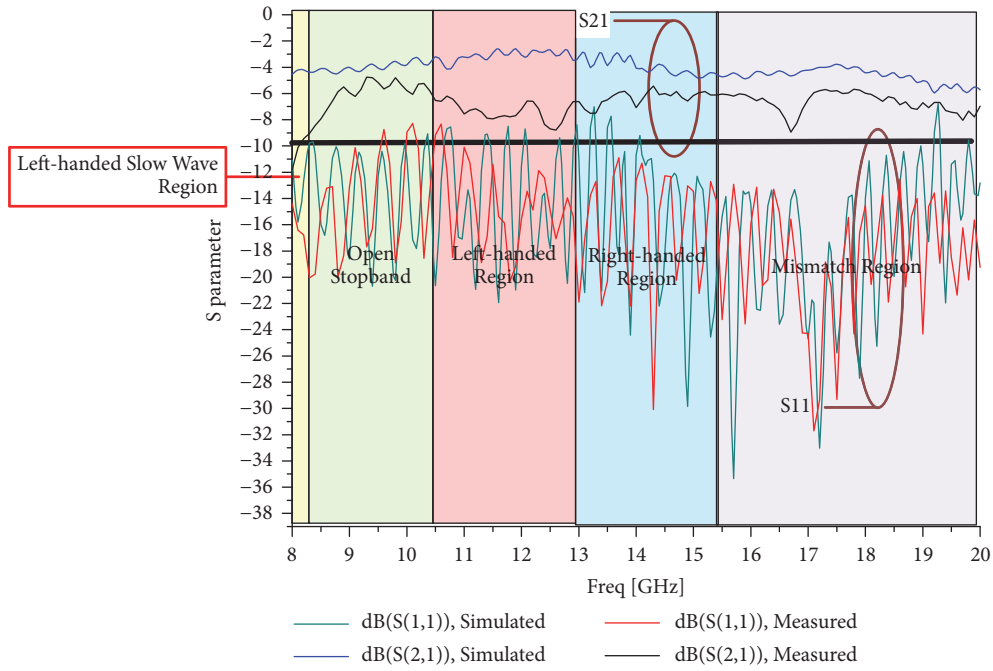

Figure 16: Simulated and measured results of S parameters of proposed antenna.

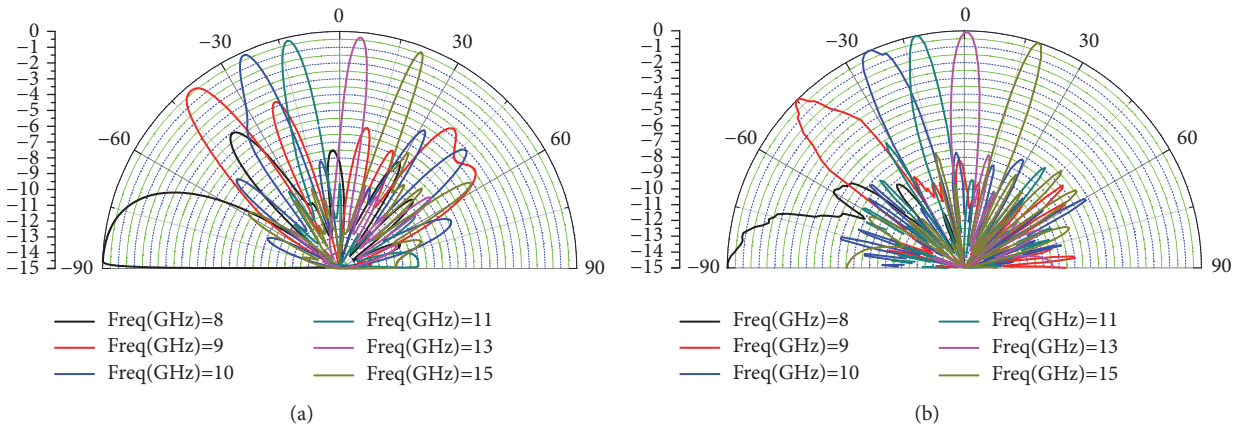

Figure 17: φ=0° plane simulated and measured results of antenna. (a) Simulated result. (b) Measured result.

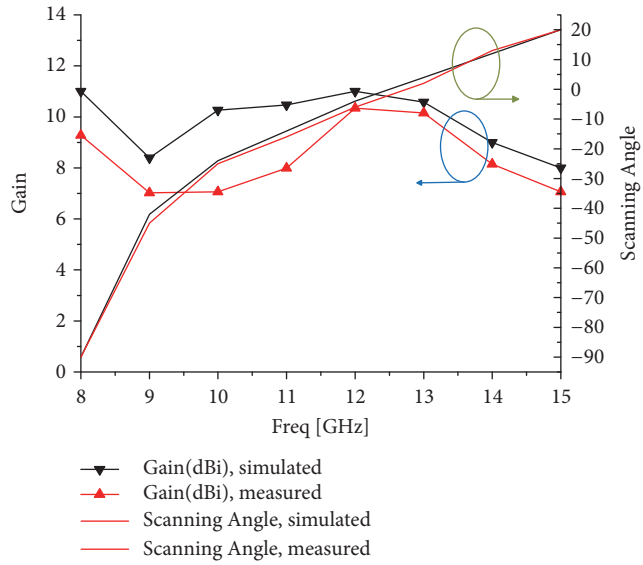

Figure 18: Gain and scanning angle of the proposed antenna.

Acknowledgments

This work was supported by the Natural Science Foundation of China (61471094).

References

[1] A. P. Hibbins, B. R. Evans, and J. R. Sambles, "Physics: Experimental verification of designer surface plasmons," *Science*, vol. 308, no. 5722, pp. 670–672, 2005.

[2] F. J. Garcia-Vidal, L. Martín-Moreno, and J. B. Pendry, "Surfaces with holes in them: new plasmonic metamaterials," *Journal of Optics A: Pure and Applied Optics*, vol. 7, no. 2, pp. S97–S101, 2005.

[3] X. Shen, T. J. Cui, D. Martin-Cano, and F. J. Garcia-Vidal, "Conformal surface plasmons propagating on ultrathin and flexible films," *Proceedings of the National Acadamy of Sciences of the United States of America*, vol. 110, no. 1, pp. 40–45, 2013.

[4] X. Shen and T. Jun Cui, "Planar plasmonic metamaterial on a thin film with nearly zero thickness," *Applied Physics Letters*, vol. 102, no. 21, article no 83, 2013.

[5] L. Shen, X. Chen, and T.-J. Yang, "Terahertz surface plasmon polaritons on periodically corrugated metal surfaces," *Optics Express*, vol. 16, no. 5, pp. 3326–3333, 2008.

[6] G. Nemova and R. Kashyap, "Theoretical model of a planar waveguide refractive index sensor assisted by a corrugated long period metal grating," *Optics Communications*, vol. 281, no. 6, pp. 1522–1528, 2008.

[7] J. J. Wu, D. J. Hou, T. J. Yang, I. J. Hsieh, Y. H. Kao, and H. E. Lin, "Bandpass filter based on low frequency spoof surface plasmon polaritons," *IEEE Electronics Letters*, vol. 48, no. 5, pp. 269-270, 2012.

[8] B. Xiao, S. Kong, J. Chen, and M. Gu, "A microwave power divider based on spoof surface plasmon polaritons," *Optical and Quantum Electronics*, vol. 48, no. 3, article no 179, 2016.

[9] Y. Fan, J. Wang, Y. Li et al., "Frequency-scanning radiation by decoupling spoof surface plasmon polaritons via phase gradient metasurface," *IEEE Transactions on Antennas and Propagation*, vol. 66, no. 1, pp. 203–208, 2018.

[10] A. Kandwal, Q. Zhang, X.-L. Tang, L. W. Liu, and G. Zhang, "Low-profile spoof surface plasmon polaritons traveling-wave antenna for near-endfire radiation," *IEEE Antennas and Wireless Propagation Letters*, vol. 17, no. 2, pp. 184–187, 2018.

[11] X. Liu, B. Chen, J. Zhang et al., "Frequency scanning planar antenna based on spoof surface plasmon polariton," *IEEE Antennas & Wireless Propagation Letters*, vol. 16, no. 99, 2017.

[12] D. Wei, J. Li, J. Yang, Y. Qi, and G. Yang, "Wide-scanning-angle leaky-wave array antenna based on microstrip SSPPs-TL," in *Proceedings of the IEEE Antennas and Wireless Propagation Letters*, vol. 17, no. 8, pp. 1566–1570, 2018.

[13] J. Wu, L. Shen, D Hou et al., "High-directivity radiation based on the leaky mode of spoof surface plasmon polaritons," *Microwaves Antennas & Propagation Iet*, vol. 8, no. 13, pp. 1075–1079, 2014.

[14] D. Guan, P. You, Q. Zhang, Z. Lu, S. Yong, and K. Xiao, "A wide-angle and circularly polarized beam-scanning antenna based on microstrip spoof surface plasmon polariton transmission line," in *Proceedings of the IEEE Antennas and Wireless Propagation Letters*, vol. 16, pp. 2538–2541, 2017.

[15] C. Zhou, L. Geng, and J. G. Liang, "A design of a compact circularly polarized patch antenna based on composite right/left-handed transmission line," *Journal of Air Force Engineering University*, 2014.

[16] Eggermont, Stephanie, and I. Huynen, "Influence of number of split rings on the leaky radiation of a metamaterial transmission line based on complementary split ring resonators," *Microwave & Optical Technology Letters*, vol. 54.4, pp. 867–875, 2012.

[17] H. Lee, J. H. Choi, C.-T. M. Wu, and T. Itoh, "A compact single radiator CRLH-inspired circularly polarized leaky-wave antenna based on substrate-integrated waveguide," *IEEE Transactions on Antennas and Propagation*, vol. 63, no. 10, pp. 4566–4572, 2015.

[18] Y. Dong and T. Itoh, "Composite right/left-handed substrate integrated waveguide and half mode substrate integrated waveguide leaky-wave structures," in *Proceedings of the IEEE Transactions on Antennas and Propagation*, vol. 59, no. 3, pp. 767–775, 2011.

[19] J. Y. Yin, J. Ren, Q. Zhang et al., "Frequency-controlled broad-angle beam scanning of patch array fed by spoof surface plasmon polaritons," *IEEE Transactions on Antennas and Propagation*, vol. 64, no. 12, pp. 5181–5189, 2016.

[20] Q. Zhang, Q. Zhang, and Y. Chen, "Spoof surface plasmon polariton leaky-wave antennas using periodically loaded patches above PEC and AMC ground planes," *IEEE Antennas and Wireless Propagation Letters*, vol. 16, pp. 3014–3017, 2017.

[21] D. Liao, Y. Zhang, and H. Wang, "Wide-angle frequency-controlled beam-scanning antenna fed by standing wave based on the cutoff characteristics of spoof surface plasmon polaritons," in *Proceedings of the IEEE Antennas and Wireless Propagation Letters*, vol. 17, no. 7, pp. 1238–1241, 2018.